

Disordered electron liquid in double quantum well heterostructures: Renormalization group analysis and dephasing rate

I.S. Burmistrov¹, I.V. Gornyi^{2,3}, and K.S. Tikhonov^{4,1}

¹*L.D. Landau Institute for Theoretical Physics, Russian Academy of Sciences, 117940 Moscow, Russia*

²*Institut für Nanotechnologie, Karlsruhe Institute of Technology, 76021 Karlsruhe, Germany*

³*A.F.Ioffe Physico-Technical Institute, 194021 St.Petersburg, Russia and*

⁴*Department of Physics, Texas A&M University, College Station, TX 77843, USA*

(Dated: June 13, 2018)

We report a detailed study of the influence of the electron-electron interaction on physical observables (conductance, etc.) of a disordered electron liquid in double quantum well heterostructure. We find that even in the case of common elastic scattering off electrons in both quantum wells, the asymmetry in the electron-electron interaction across and within quantum wells decouples them at low temperatures. Our results are in quantitative agreement with recent transport experiments on the gated double quantum well $\text{Al}_x\text{Ga}_{1-x}\text{As}/\text{GaAs}/\text{Al}_x\text{Ga}_{1-x}\text{As}$ heterostructures.

PACS numbers: 72.10.-d 71.30.+h, 73.43.Qt 11.10.Hi

I. INTRODUCTION

Disordered two-dimensional (2D) electronic systems have been remaining in the focus of experimental and theoretical research for more than three decades.¹ The experimental discovery^{2,3} of the metal-insulator transition (MIT) in a high mobility silicon metal-oxide-semiconductor field-effect transistor (Si-MOSFET) in 1994 became a challenge to a theory. Although during last decade the behavior of resistivity similar to that of Ref. [2,3] has been found experimentally in a wide variety of two-dimensional electron systems,⁴ the MIT in two dimensions still calls for deeper theoretical and experimental understanding.

Very likely, the most promising theoretical framework for studying the 2D MIT is provided by the effective low-energy theory, initially developed by Finkelstein, that combines the diffusive dynamics due to disorder and strong electron-electron interaction.⁵ Moreover, it is the Finkelstein theory that suggested metallic behavior at low temperatures long before the experimental discovery of the MIT in a Si-MOSFET.^{5,6} Recently, Punnoose and Finkelstein⁷ have shown a possibility for the existence of the MIT in the special model of 2D electron system with $SU(\mathcal{N})$ degrees of freedom in the limit of the large number of multiplets, $\mathcal{N} \rightarrow \infty$. On the other hand, the current theoretical results^{8,9} do not support the existence of MIT for electrons interacting in the singlet channel only ($\mathcal{N} = 1$). Therefore, the presence of additional degrees of freedom (spins, valley isospins etc.) plays a crucial role for the existence of the MIT in 2D disordered electron systems. In fact, the importance of the multiplet channels of the interaction has been confirmed experimentally in Si-MOSFET where a weak magnetic field applied parallel to the 2D plane changes the behavior of resistivity from metallic to insulating at low temperatures.¹⁰⁻¹² These experimental findings have been explained in framework of the Finkelstein theory in the presence of Zeeman and valley splitting.¹³ The effect of intervalley scattering has been taken into account as

well.¹⁴

Recently, the Finkelstein theory for disordered electron liquid in Si-MOSFET has been subjected to a detailed experimental check. In particular, the metallic behavior of resistivity not far away from the MIT,¹⁵ the increase of interaction parameter in the multiplet channels,¹⁶⁻¹⁸ and the two-parameter scaling near MIT¹⁹ have been observed in experiments. Such the analysis in Si-MOSFET is complicated by the presence of (uncontrolled) large valley splitting and intervalley scattering rate, $\Delta_v \approx 1/\tau_v \approx 1K$.^{20,21}

As known,²² in n-AlAs quantum wells, 2D electrons can also populate two valleys. In addition to Si-MOSFETs this system offers opportunity for an experimental investigation of the interplay between the spin and valley degrees of freedom. Using a symmetry breaking strain to tune the valley occupation of the 2D electron system in the n-AlAs quantum well, as well as a parallel magnetic field to adjust the spin polarization, the spin – valley interplay has been experimentally studied.^{23,24} However, the electron concentrations in the experiment were at least three times larger than the critical one corresponding to the MIT.²² Therefore, the spin-valley interplay in n-AlAs quantum well has been studied only in the region of a good metal, very far from the MIT.

Disordered electron liquid in double quantum well heterostructures represents a 2D system in which electrons in addition to spin have the other degree of freedom: the isospin associated with a quantum well. In spite of a number of interesting physical phenomena observed in electron liquids in double quantum well heterostructures without and under strong magnetic field, e.g., Coulomb drag,²⁵ Bose-Einstein condensation of excitons²⁶, ferromagnetic²⁷ and canted antiferromagnetic phases,²⁸ the metal-insulator transition has not been yet addressed experimentally. Transport of electrons in double quantum well heterostructures has been studied experimentally^{29,30} only in the metallic regime far from the region in which MIT is expected.

Recently, detailed experimental research on the in-

interference and interaction corrections to conductance of electrons in a double quantum well heterostructure has been performed.^{31,32} In particular, two very distinct physical situations have been investigated: i) both quantum wells have equal electron concentrations and mobilities; ii) one quantum well remains with almost the same electron concentration as in case i), whereas the other is empty by applying the gate voltage. Surprisingly, it was found that the dephasing rate and interaction correction to the conductance are almost the same for cases i) and ii).

In the present paper, motivated by the experiments of Refs. [31,32], we develop the theory of the disordered electron liquid formed in a heterostructure with two almost identical quantum wells. We concentrate on the case of equal electron concentrations and mobilities in both quantum wells [corresponding to the case i) of Refs. 31,32]. This case will be termed as balance in what follows.

We restrict our study to temperatures (T) satisfying the following condition: $1/\tau_{+-}, \Delta_s, \Delta_{SAS} \ll T \ll 1/\tau_{tr}$. Here $1/\tau_{+-}$ stands for the rate of elastic scattering between symmetric and antisymmetric states in the double quantum well structure, Δ_{SAS} the splitting of these symmetric and antisymmetric states, Δ_s the Zeeman splitting, and τ_{tr} the elastic transport mean free time. The temperature behavior of the interaction correction to the total conductance is governed by one singlet and 15 multiplet diffusive modes. We find that the latter splits into three inequivalent groups of one, six, and eight modes. This grouping occurs due to asymmetry in electron-electron interactions across and within quantum wells which breaks the rotational symmetry in the combined spin and isospin spaces [$SU(4)$]. This reduced symmetry is a distinctive feature of double quantum well heterostructures at the balance and is absent in two-valley systems in Si-MOSFETs and n-AlAs quantum wells. We identify all relevant interaction parameters and estimate their dependence on the distance between the quantum wells. To describe the system at low temperatures and beyond interaction corrections to conductance, we derive the non-linear sigma model and study its renormalization in the one-loop approximation. As we demonstrate, the renormalization group equations describing the length scale dependence of the total conductance and interaction parameters drive the system towards the fixed point corresponding to two separate quantum wells. In spite of the symmetry breaking between 15 multiplet modes, the renormalization group equations predict the metallic behavior of the conductance at low temperatures. Finally, we generalize the expression for the dephasing rate of electrons due to the presence of electron-electron interaction known^{33,34} for a single quantum well to the case of double quantum well heterostructures. We find that our results are in good quantitative agreement with experimental data of Refs. [31,32].

The paper is organized as follows. In Section II we introduce the microscopic Hamiltonian, identify relevant

interaction parameters, study its dependence on the distance between quantum wells and introduce the nonlinear sigma model that describes the low-energy excitations in the disordered interacting electron system. Then, in Sec. III we consider the renormalization of the nonlinear sigma model in the one-loop approximation, derive corresponding renormalization group equations, and discuss renormalization group flow. We derive expressions for the dephasing rate due to electron-electron interactions in Sec. IV. Next in Sec. V we perform detailed comparison between our theory and recent experimental data on transport in double quantum well heterostructures. We end the paper with conclusions (Sec. VI).

II. FORMALISM

A. Microscopic Hamiltonian

We consider 2D interacting electrons in double quantum well heterostructures in the presence of quenched disorder at low temperatures $T \ll \tau_{tr}^{-1}$. In the case of two almost identical quantum wells an electron annihilation operator can be written as a linear combination of symmetric and antisymmetric states:

$$\psi^\sigma(\mathbf{R}) = \psi_\tau^\sigma(\mathbf{r})\varphi_\tau(z), \quad \varphi_\tau(z) = \frac{\varphi_l(z) + \tau\varphi_r(z)}{\sqrt{2}}. \quad (1)$$

Here electron motion along z axis is confined by the quantum wells, \mathbf{r} denotes a vector in plane perpendicular to the z axis, and $\mathbf{R} = \mathbf{r} + z\mathbf{e}_z$. The superscript $\sigma = \pm$ denotes electron spin projection, $\tau = \pm$ enumerates symmetric (+) and antisymmetric (-) states in the double quantum well structure and ψ_τ^σ is the annihilation operator of an electron with the spin and isospin projections equal $\sigma/2$ and $\tau/2$, respectively. The normalized envelope function $\varphi_{l,r}(z) = \varphi(z \pm d/2)$ corresponds to the wave function of an electron localized in a single left/right well. In what follows, we assume a negligible overlap between the states in two quantum wells: the width of an electron state in a quantum well $[\int dz \varphi^4(z)]^{-1} \ll d$ where d is the distance between the centers of the quantum wells.

In the path-integral formulation, interacting electrons in the presence of the random potential $V(\mathbf{R})$ are described by the following grand partition function

$$Z = \int \mathcal{D}[\bar{\psi}, \psi] e^{\mathcal{S}[\bar{\psi}, \psi]} \quad (2)$$

with the imaginary time action ($\beta = 1/T$)

$$S = - \int_0^\beta dt \left\{ \int d\mathbf{r} \bar{\psi}_\tau^\sigma(\mathbf{r}t) [\partial_t + \mathcal{H}_0] \psi_\tau^\sigma(\mathbf{r}t) - \mathcal{L}_{\text{dis}} - \mathcal{L}_{\text{int}} \right\}. \quad (3)$$

The single-particle Hamiltonian

$$\mathcal{H}_0 = -\frac{\nabla^2}{2m_e} - \mu + \frac{1}{2}(\Delta_s\sigma + \Delta_{SAS}\tau) \quad (4)$$

describes a 2D quasiparticle with mass m_e . Magnetic field B perpendicular to the z axis induces the Zeeman splitting $\Delta_s = g\mu_B B$. The energy difference between symmetric and antisymmetric states in a double quantum well structure yields the splitting $\Delta_{SAS} \simeq 2\varphi(d/2)\varphi'(d/2)/m_e$.³⁵ The chemical potential is denoted as μ , g stands for the effective electron g -factor and μ_B the Bohr magneton. The single-particle Hamiltonian (4) is completely analogous to one for a Si(001)-MOSFET. In latter case, index τ enumerates valleys and Δ_{SAS} plays a role of a valley splitting.

Next, the term

$$\mathcal{L}_{\text{dis}} = - \int d\mathbf{r} \bar{\psi}_{\tau_1}^{\sigma}(\mathbf{r}t) V_{\tau_1\tau_2}(\mathbf{r}) \psi_{\tau_2}^{\sigma}(\mathbf{r}t) \quad (5)$$

describes electron scattering off a random potential $V(\mathbf{R})$. It involves matrix elements

$$V_{\tau_1\tau_2}(\mathbf{r}) = \int dz V(\mathbf{R}) \varphi_{\tau_1}(z) \varphi_{\tau_2}(z). \quad (6)$$

In general, the matrix elements $V_{\tau_1\tau_2}$ induce transitions between symmetric and antisymmetric states in a double quantum well structure. In the case of symmetric random potential: $V(\mathbf{r}, z) = V(\mathbf{r}, -z)$, the system is protected from the symmetric-antisymmetric scattering.

In accordance with the experimental conditions reported in Ref. [31,32], we assume that impurities are concentrated in the middle between two quantum wells. We suppose that the random potential created by impurities has the Gaussian distribution, and

$$\langle V(\mathbf{R}) \rangle = 0, \quad \langle V(\mathbf{R}_1) V(\mathbf{R}_2) \rangle = W(|\mathbf{r}_1 - \mathbf{r}_2|, |z_1|, |z_2|), \quad (7)$$

where W decays as the function of its variables at a typical distance d_W . If the condition

$$\left[\int dz \varphi^4(z) \right]^{-1} \ll d, \quad (8)$$

holds, we can neglect the small difference [proportional to $\varphi(d/2)\varphi'(d/2)$], between symmetric-symmetric and antisymmetric-antisymmetric scattering rates. Then

$$\langle V_{\tau_1\tau_2}(\mathbf{r}_1) V_{\tau_3\tau_4}(\mathbf{r}_2) \rangle = W(|\mathbf{r}_1 - \mathbf{r}_2|, d/2, d/2) \delta_{\tau_1\tau_2} \delta_{\tau_3\tau_4}. \quad (9)$$

Provided correlations in W are short-ranged,³⁷ we find

$$\langle V_{\tau_1\tau_2}(\mathbf{r}_1) V_{\tau_3\tau_4}(\mathbf{r}_2) \rangle = \frac{1}{2\pi\nu\tau_i} \delta_{\tau_1\tau_2} \delta_{\tau_3\tau_4} \delta(\mathbf{r}_1 - \mathbf{r}_2), \quad (10)$$

$$\frac{1}{\tau_i} = 2\pi\nu \int d^2\mathbf{r} W(|\mathbf{r}|, d/2, d/2).$$

Here ν is the thermodynamic density of states of 2D electrons (including spin). We emphasize that electrons in both quantum wells are subjected to correlated disorder since they scatter off the very same random potential. Recently, under such assumptions, the transconductance

of a double quantum well structure (the Coulomb drag effect with correlated disorder) has been studied by one of the authors.³⁶

The small asymmetry in the impurity distribution along z axis will lead to the scattering between symmetric and antisymmetric states in the double quantum well structure. Its rate can be estimated as $1/\tau_{+-} \sim (b/d)^2/\tau_i \ll 1/\tau_i$ where b is a typical length characterizing asymmetry. We neglect $1/\tau_{+-}$ in what follows.

The interaction part of the action (3) reads

$$\mathcal{L}_{\text{int}} = -\frac{1}{2} \int d\mathbf{R} d\mathbf{R}' \rho(\mathbf{R}t) U(|\mathbf{R} - \mathbf{R}'|) \rho(\mathbf{R}'t) \quad (11)$$

where $U(\mathbf{R}) = e^2/\epsilon R$. The dielectric constant is denoted as ϵ . Expanding the density operator $\rho(\mathbf{R}t) = \bar{\psi}_{\tau_1}^{\sigma}(\mathbf{r}t) \psi_{\tau_2}^{\sigma}(\mathbf{r}t) \varphi_{\tau_1}(z) \varphi_{\tau_2}(z)$ and assuming again that condition (8) holds we obtain

$$\mathcal{L}_{\text{int}} = -\frac{1}{8} \int d\mathbf{r} d\mathbf{r}' \bar{\psi}_{\tau_1}^{\sigma_1}(\mathbf{r}t) \psi_{\tau_2}^{\sigma_1}(\mathbf{r}t) \bar{\psi}_{\tau_3}^{\sigma_2}(\mathbf{r}'t) \psi_{\tau_4}^{\sigma_2}(\mathbf{r}'t) \times \left[(1 + \tau_1\tau_2\tau_3\tau_4) U_{11}(|\mathbf{r} - \mathbf{r}'|) + (\tau_1\tau_2 + \tau_3\tau_4) U_{12}(|\mathbf{r} - \mathbf{r}'|) \right]. \quad (12)$$

Here

$$U_{11}(r) = \frac{e^2}{\epsilon} \int dz dz' \frac{\varphi_l^2(z) \varphi_l^2(z')}{\sqrt{r^2 + (z - z')^2}} \approx \frac{e^2}{\epsilon r} \quad (13)$$

is the standard Coulomb interaction between electrons in a single well. The interaction between electrons in different quantum wells

$$U_{12}(r) = \frac{e^2}{\epsilon} \int dz dz' \frac{\varphi_l^2(z) \varphi_r^2(z')}{\sqrt{r^2 + (z - z')^2}} \approx \frac{e^2}{\epsilon \sqrt{r^2 + d^2}} \quad (14)$$

takes into account that electrons are separated by the distance d . Due to the difference between U_{11} and U_{12} the interaction Lagrangian \mathcal{L}_{int} is not invariant under global $SU(4)$ rotations of the electron operator ψ_{τ}^{σ} in the combined spin-isospin space. It is the interaction part of the action (3) that distinguishes the disordered electron liquid in double quantum well heterostructures from the one in a Si(001)-MOSFET.

As usual, we single out regions in the momentum space of small momentum transfer^{5,6,38,39}. Then the low energy part of \mathcal{L}_{int} can be written as

$$\mathcal{L}_{\text{int}} = \frac{1}{4\nu} \int' \frac{d\mathbf{q}}{(2\pi)^2} \sum_{a,b=0}^3 \mathbb{F}_{ab}(q) m^{ab}(\mathbf{q}) m^{ab}(-\mathbf{q}), \quad (15)$$

$$m^{ab}(\mathbf{q}) = \int \frac{d\mathbf{k}}{(2\pi)^2} \bar{\psi}(\mathbf{k} + \mathbf{q}) t_{ab} \psi(\mathbf{k}). \quad (16)$$

Here $\bar{\psi} = \{\bar{\psi}_+^{\pm}, \bar{\psi}_-^{\pm}\}$, $\psi = \{\psi_+^{\pm}, \psi_-^{\pm}\}^T$, the ‘prime’ at the integral sign denotes the integration region $q \lesssim l^{-1}$ (l is the elastic mean free path), and 16 matrices $t_{ab} = \tau_a \otimes \sigma_b$ stand for the generators of $SU(4)$.

Pauli matrices τ_a , $a = 0, 1, 2, 3$ act in the isospin space of two wells and Pauli matrices σ_b , $b = 0, 1, 2, 3$ act in the spin space. The matrix of interaction parameters reads

$$\mathbb{F}(q) = \begin{pmatrix} F_s & F_t & F_t & F_t \\ \tilde{F}_s & F_t & F_t & F_t \\ F_v & F_v & F_v & F_v \\ F_v & F_v & F_v & F_v \end{pmatrix} \quad (17)$$

where

$$\begin{aligned} F_t &= -\frac{\nu}{2} \langle U_{11}^{\text{scr}}(0) \rangle_{FS}, & F_v &= -\frac{\nu}{2} \langle U_{12}^{\text{scr}}(0) \rangle_{FS}, \\ F_s &= \nu[U_{11}(q) + U_{12}(q)] + F_t, \\ \tilde{F}_s &= \nu[U_{11}(q) - U_{12}(q)] + F_t. \end{aligned} \quad (18)$$

Here $U_{11}(q) = 2\pi e^2/q\epsilon$, $U_{12}(q) = U_{11}(q) \exp(-qd)$. The quantities F_t and F_v are analogous to the standard Fermi liquid interaction parameters in the triplet channel. They involve averaging of the static part of dynamically screened interaction $U_{11/12}^{\text{scr}}(q, \omega)$ over the Fermi surface. In the case of equal electron concentrations and mobilities in both quantum wells

$$\langle U_{11/12}^{\text{scr}}(0) \rangle_{FS} = \int_0^{2\pi} \frac{d\theta}{2\pi} U_{11/12}^{\text{scr}}(2k_F \sin(\theta/2), 0) \quad (19)$$

where k_F is Fermi momentum for a single quantum well. The interaction parameter F_s involves the long-range part of the Coulomb interaction. In the limit $q \rightarrow 0$ it becomes $F_s(q) \approx 2\kappa/q \rightarrow \infty$ where $\kappa = 2\pi e^2\nu/\epsilon$. Within the same accuracy, we find

$$\tilde{F}_s = \kappa d + F_t. \quad (20)$$

At $d = 0$ —when both quantum wells coincide—the interaction parameters are equal: $\tilde{F}_s = F_t = F_v$. Then the matrix \mathbb{F} corresponds to the case of electron liquid with two valleys as it occurs in Si(001)-MOSFET. In the absence of Δ_{SAS} and Δ_s the action (3) becomes invariant under global $SU(4)$ rotations of the fermionic fields. In the opposite case of $d \rightarrow \infty$, the double quantum well heterostructure is equivalent to two independent single quantum wells. Then we obtain $\tilde{F}_s = F_s$, and $F_v = 0$. The action (3) (for $\Delta_{SAS} = \Delta_s = 0$) becomes invariant under global $SU(2)$ rotations of electron spin in each quantum well independently. For intermediate values of d , the action (3) is also invariant under global $SU(2) \times SU(2)$ rotations provided Δ_{SAS} and Δ_s vanish.

B. Dynamically screened Coulomb interaction

The interaction parameters F_t and F_v involve the screened Coulomb interaction. Solving the Dyson equations in the random phase approximation (RPA) (see Fig. 1), we obtain the following results for the dynam-

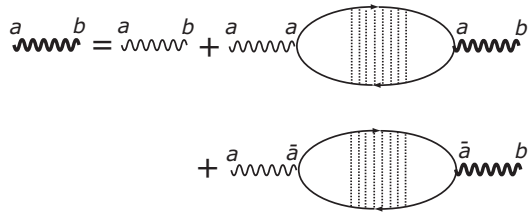


FIG. 1: Dyson equation for the screened electron-electron interaction in RPA. Thick wavy line denotes screened interaction, thin wavy line is bare interaction, solid lines are electron Green's functions, and dashed lines are impurity lines. Indices a and b can be 1 or 2. Index \bar{a} equals 1 (2) if index a is 2 (1).

ically screened interactions:^{40,41}

$$U_{11}^{\text{scr}} = \frac{U_{11} + \Pi_2[U_{11}^2 - U_{12}^2]}{1 + [\Pi_1 + \Pi_2]U_{11} + \Pi_1\Pi_2[U_{11}^2 - U_{12}^2]}, \quad (21)$$

$$U_{12}^{\text{scr}} = \frac{U_{12}}{1 + [\Pi_1 + \Pi_2]U_{11} + \Pi_1\Pi_2[U_{11}^2 - U_{12}^2]}, \quad (22)$$

$$U_{22}^{\text{scr}} = \frac{U_{11} + \Pi_1[U_{11}^2 - U_{12}^2]}{1 + [\Pi_1 + \Pi_2]U_{11} + \Pi_1\Pi_2[U_{11}^2 - U_{12}^2]}. \quad (23)$$

The polarization operators can be written in diffusive approximation as

$$\Pi_j(q, \omega) = \nu \frac{D_j q^2}{D_j q^2 - i\omega}, \quad j = 1, 2 \quad (24)$$

where D_j is the diffusion coefficient in the j -th quantum well. We mention that for $D_1 \neq D_2$ the dynamically screened Coulomb interaction in the first well $U_{11}^{\text{scr}}(q, \omega)$ does not coincide with the one ($U_{22}^{\text{scr}}(q, \omega)$) in the second well.

If the electron concentrations and mobilities in the quantum wells are the same then $D_1 = D_2$. In this case $U_{11}^{\text{scr}} = U_{22}^{\text{scr}}$ and

$$\begin{aligned} U_{11/12}^{\text{scr}} &= \frac{\kappa}{2\nu q} (Dq^2 - i\omega) \left\{ \frac{1 + e^{-qd}}{Dq [q + \kappa(1 + e^{-qd})] - i\omega} \right. \\ &\quad \left. \pm \frac{1 - e^{-qd}}{Dq [q + \kappa(1 - e^{-qd})] - i\omega} \right\}. \end{aligned} \quad (25)$$

As one can see, at $qd \gg 1$ the effect of the right well on the dynamically screened interaction in the left well is negligible. In the opposite case, $qd \ll 1$ the right well affects the dynamically screened interaction in the left well only at $\kappa d \lesssim 1$.

C. Estimates for the interaction parameters

Let us estimate the interaction parameters F_t and F_v in the case of equal electron concentrations in both quantum

wells. By using Eqs. (21) and (22) we find

$$F_t \pm F_v = - \int_0^{2\pi} \frac{d\theta}{4\pi} \frac{\varkappa(1 \pm e^{-2k_F d \sin \theta/2})}{2k_F \sin \frac{\theta}{2} + \varkappa(1 \pm e^{-2k_F d \sin \theta/2})}. \quad (26)$$

To justify the RPA which has been used in derivation of Eqs. (21)-(22) we assume that the condition $\varkappa/k_F \ll 1$ holds. As follows from Eq. (26), both F_t and F_v are negative and $|F_t| \geq |F_v|$. The interaction parameter \tilde{F}_s is negative at small d and positive at large d . The dependence of the critical distance d_c at which \tilde{F}_s vanishes on the parameter \varkappa/k_F is shown in Fig. 2. We mention that $|\tilde{F}_s| \leq |F_t|$ for $d < d_c$.

It is instructive to compare the results for F_t , F_v and \tilde{F}_s with the case of a single quantum well for which the interaction parameter in the triplet channel is given as³⁹

$$F_t^0 = - \int_0^{2\pi} \frac{d\theta}{4\pi} \frac{\varkappa}{2k_F \sin(\theta/2) + \varkappa} = - \frac{1}{2\pi} \mathcal{G}_0(\varkappa/2k_F),$$

$$\mathcal{G}_0(x) = \frac{x}{\sqrt{1-x^2}} \ln \frac{1 + \sqrt{1-x^2}}{1 - \sqrt{1-x^2}}. \quad (27)$$

In the limit $x \rightarrow 0$ the function $\mathcal{G}_0(x)$ acquires the following asymptotic form

$$\mathcal{G}_0(x) \approx x \ln(2/x), \quad x \ll 1. \quad (28)$$

Provided $k_F d \gg 1$, the interaction parameters for the case of double quantum wells with equal electron concentrations can be estimated as

$$F_t = F_t^0 + \frac{1}{8\pi k_F d} \mathcal{G}_1(\varkappa d), \quad F_v = \frac{1}{8\pi k_F d} \mathcal{G}_2(\varkappa d), \quad (29)$$

$$\mathcal{G}_1(x) = \frac{3x e^x E_1(x)}{x+1} + \frac{2x e^{-2x/(x-1)} E_1\left(-\frac{2x}{x-1}\right)}{x^2-1},$$

$$\mathcal{G}_2(x) = \mathcal{G}_1(x) - \frac{4x e^x E_1(x)}{x+1}.$$

Here $E_1(x) = \int_x^\infty dt \exp(-t)/t$ is the exponential integral.

Finally, we mention that the interaction parameters F_t and F_v can be estimated (from above) as $|F_t| \leq [\mathcal{G}_0(\varkappa/k_F) + \mathcal{G}_0(\varkappa/2k_F)]/(4\pi)$ and $|F_v| \leq \mathcal{G}_0(\varkappa/k_F)/(4\pi)$. Even for values of $\varkappa/k_F \sim 1$, it yields $|F_t| \lesssim 0.3$ and $|F_v| \lesssim 0.2$.

D. Non-linear σ model

At low temperatures, $T\tau_{tr} \ll 1$, the effective quantum theory of 2D disordered interacting electrons described by the microscopic action (3) is given in terms of the non-linear sigma model. The latter describes interaction between low-energy modes which are the so-called ‘‘Diffusons’’ and ‘‘Cooperons’’. As well-known,^{33,42,43} the interference (‘‘Cooperon’’) contribution to the conductance

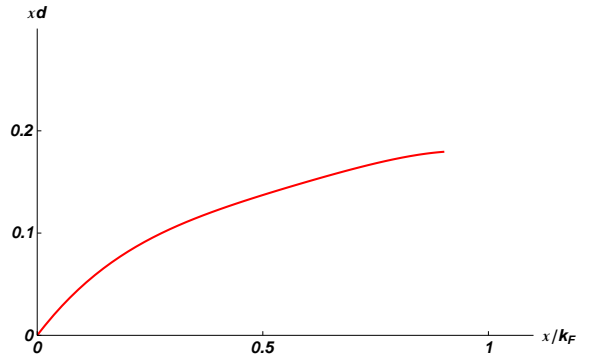


FIG. 2: Value of the parameter $\varkappa d$ at which $\tilde{F}_s = 0$ versus \varkappa/k_F .

is not sensitive to the presence of Δ_s and Δ_{SAS} (in the absence of $1/\tau_{+-}$). Furthermore, the interference correction is cut off by weak magnetic fields and does not influence the scaling of observables with temperature at $B \gtrsim 1/eD\tau_\varphi$. Therefore, we shall ignore the interference correction in the intermediate calculations for a sake of simplicity and shall discuss its role in Sec. V.

In general, Cooperons are also involved in the interaction correction to the conductance and the renormalization of other interaction couplings. The corresponding contributions are proportional to the interaction parameter in the Cooper channel. For Coulomb interaction, the latter is repulsive and remains small in the course of the renormalization for 2D electron systems.⁵ Moreover, physically, a moderately weak magnetic field $B \gtrsim T/eD$ applied parallel to the z axis is enough to suppress the interaction effects in the Cooper channel.⁴⁴

Neglecting the Cooper channel, the effective theory involves unitary matrix field variables $Q_{mn;\tau_1\tau_2}^{\alpha_1\alpha_2; \sigma_1\sigma_2}(\mathbf{r})$ which obey the nonlinear constraint $Q^2(\mathbf{r}) = 1$. The integers $\alpha_j = 1, 2, \dots, N_r$ denote the replica indices. The integers m, n correspond to the discrete set of Matsubara frequencies $\varepsilon_n = \pi T(2n + 1)$.

The effective sigma-model action is

$$\mathcal{S} = \mathcal{S}_\sigma + \mathcal{S}_F + \mathcal{S}_{SB}. \quad (30)$$

Here \mathcal{S}_σ represents the free electron part⁴⁵

$$\mathcal{S}_\sigma = - \frac{\sigma_{xx}}{32} \int d\mathbf{r} \text{tr} (\nabla Q)^2 \quad (31)$$

with $\sigma_{xx} = 4\pi\nu_*D$ denoting the mean-field conductance in units of e^2/h . The thermodynamic density of states $\nu_* = m_*/\pi$ involves an effective mass m_* renormalized due to interactions. The symbol tr stands for the trace over replica, the Matsubara frequencies, spin and isospin indices. The Finkelstein term^{5,46}

$$\mathcal{S}_F = - \frac{\pi T}{4} \int d\mathbf{r} \sum_{an;ab} \Gamma_{ab} \text{tr} I_n^\alpha t_{ab} Q(\mathbf{r}) \text{tr} I_{-n}^\alpha t_{ab} Q(\mathbf{r})$$

$$+ 4\pi T z \int d\mathbf{r} \text{tr} \eta(Q - \Lambda) - 2\pi T z \int d\mathbf{r} \text{tr} \eta \Lambda \quad (32)$$

involves the electron-electron interaction amplitudes Γ_{ab} . The bare value of the factor z is determined by the thermodynamic density of states: $z = \pi\nu_*/4$. The quantity z has been originally introduced by Finkelstein in order to ensure the consistence of the renormalization group equations with the particle number conservation.⁵ Physically, the renormalization of z is responsible for renormalization of the specific heat⁴⁷ and determines the relation between the frequency and length scales, thus playing a crucial role at the criticality near the MIT.⁵

The interaction amplitudes Γ_{ab} are related to the interaction parameters \mathbb{F}_{ab} introduced above as^{5,6,38} $\Gamma_{ab} = -z\mathbb{F}_{ab}/(1 + \mathbb{F}_{ab})$. Therefore, the matrix Γ has the structure similar to the matrix \mathbb{F} (see Eq. (17)) and

$$\begin{aligned} \Gamma_s &= -z, \quad \tilde{\Gamma}_s = -z\tilde{\gamma}_s, \quad \Gamma_t = -z\gamma_t, \quad \Gamma_v = -z\gamma_v, \\ \tilde{\gamma}_s &= -\frac{\tilde{F}_s}{1 + \tilde{F}_s}, \quad \gamma_t = -\frac{F_t}{1 + F_t}, \quad \gamma_v = -\frac{F_v}{1 + F_v}. \end{aligned} \quad (33)$$

The matrices Λ , η and I_k^γ are given as

$$\begin{aligned} \Lambda_{nm}^{\alpha\beta} &= \text{sign}(\omega_n)\delta_{nm}\delta^{\alpha\beta}t_{00}, \quad \eta_{nm}^{\alpha\beta} = n\delta_{nm}\delta^{\alpha\beta}t_{00}, \\ (I_k^\gamma)_{nm}^{\alpha\beta} &= \delta_{n-m,k}\delta^{\alpha\gamma}\delta^{\beta\gamma}t_{00}. \end{aligned} \quad (34)$$

The action $\mathcal{S}_\sigma + \mathcal{S}_F$ is invariant under the global rotations $Q_{nm;\tau_1\tau_2}^{\alpha\beta;\sigma_1\sigma_2}(\mathbf{r}) \rightarrow u_{\sigma_1\tau_1}^{\tau_3} Q_{nm;\tau_3\tau_4}^{\alpha\beta;\sigma_3\sigma_4}(\mathbf{r})[u^{-1}]_{\sigma_4\tau_2}^{\tau_4}$ with $u = \sum_{a=0}^1 \sum_{b=0}^3 u_{ab}t_{ab}$. This rotation correspond to the global $SU(2) \times SU(2)$ symmetry of the action $\mathcal{S}_\sigma + \mathcal{S}_F$.

The presence of Δ_s and/or Δ_{SAS} generates the symmetry breaking terms. In general, they can be written as⁵

$$\mathcal{S}_{SB} = iz_{ab}\Delta_{ab} \int d\mathbf{r} \text{tr} t_{ab}Q + \frac{N_r z_{ab}}{\pi T} \int d\mathbf{r} \Delta_{ab}^2. \quad (35)$$

For the symmetry breaking by the Zeeman splitting one can choose $t_{ab} = t_{03}$ and $\Delta_{03} = \Delta_s$. In the case of the splitting Δ_{SAS} , the generator t_{ab} equals t_{30} . Splitting Δ_{ab} set the cut-off for a pole in the diffusion modes (“dif-fusons”). In what follows, we shall be interested in high temperatures ($T \gg \Delta_{ab}$) or, correspondingly, in short length scales $L \ll \sqrt{D/\Delta_{ab}}$ such that the cut-off is irrelevant and the electron system behaves as if no symmetry breaking terms are exist. We shall use the symmetry breaking term \mathcal{S}_{SB} only as a source, assuming infinitesimal Δ_{ab} .

1. \mathcal{F} -algebra

The action (30) involves the matrices which are formally defined in the infinite Matsubara frequency space. In order to operate with them we have to introduce a cut-off for the Matsubara frequencies. One should send the cut-off to infinity at the end of all calculations. Then, the set of rules which is called \mathcal{F} -algebra can be established.⁴⁶ The global rotations of Q with the matrix $\exp(i\hat{\chi})$ where

$\hat{\chi} = \sum_{\alpha,n} \chi_n^\alpha I_n^\alpha$ play the important role.^{46,48} For example, \mathcal{F} -algebra allows us to establish the following relations

$$\begin{aligned} \text{tr} I_n^\alpha t_{ab} e^{i\hat{\chi}} Q e^{-i\hat{\chi}} &= \text{tr} I_n^\alpha t_{ab} e^{i\chi_0} Q e^{-i\chi_0} + 8in(\chi_{ab})_{-n}^\alpha, \\ \text{tr} \eta e^{i\hat{\chi}} Q e^{-i\hat{\chi}} &= \text{tr} \eta Q + \sum_{\alpha n; ab} in(\chi_{ab})_n^\alpha \text{tr} I_n^\alpha t_{ab} Q \\ &\quad - 4 \sum_{\alpha n; ab} n^2 (\chi_{ab})_n^\alpha (\chi_{ab})_{-n}^\alpha \end{aligned} \quad (36)$$

where $\chi_0 = \sum_\alpha \chi_0^\alpha I_0^\alpha$. With the help of Eqs. (36) one can check that the relation $\Gamma_s = -z$ guarantees the so-called \mathcal{F} -invariance.⁴⁶ It is the invariance of the action $\mathcal{S}_\sigma + \mathcal{S}_F$ under the global rotation of the matrix Q with $\chi_{ab} = \chi\delta_{a0}\delta_{b0}$.

E. Physical observables

The most significant physical quantities in the theory containing information on its low-energy dynamics are physical observables σ'_{xx} , z' , and z'_{ab} associated with the mean-field parameters σ_{xx} , z , and z_{ab} of the action (30). The observable σ'_{xx} is the total DC conductance as obtained from the linear response to an electromagnetic field. The observable z' is related with the specific heat.⁴⁷ The observables z_{ab} determine the static generalized susceptibilities of the 2D electron system^{5,49} as $\chi_{ab} = 2z'_{ab}/\pi$. The conductance σ'_{xx} can be obtained from

$$\begin{aligned} \sigma'_{xx}(i\omega_n) &= -\frac{\sigma_{xx}}{16n} \langle \text{tr} [I_n^\alpha, Q] [I_{-n}^\alpha, Q] \rangle \\ &\quad + \frac{\sigma_{xx}^2}{64\mathbb{D}n} \int d\mathbf{r}' \langle \langle \text{tr} I_n^\alpha Q(\mathbf{r}) \nabla Q(\mathbf{r}) \text{tr} I_{-n}^\alpha Q(\mathbf{r}') \nabla Q(\mathbf{r}') \rangle \rangle \end{aligned} \quad (37)$$

after the analytic continuation to the real frequencies: $i\omega_n \rightarrow \omega + i0^+$ at $\omega \rightarrow 0$. The expectation values are defined with respect to the theory (30) and $\mathbb{D} = 2$ stands for the spatial dimension. The physical observable z' can be extracted from the derivative of the thermodynamic potential Ω per the unit volume with respect to temperature,⁴⁶

$$z' = \frac{1}{2\pi \text{tr} \eta \Lambda} \frac{\partial}{\partial T} \frac{\Omega}{T}. \quad (38)$$

The observables z'_{ab} are given as

$$z'_{ab} = \frac{\pi}{2N_r} \frac{\partial^2 \Omega}{\partial \Delta_{ab}^2} \Big|_{\Delta_{ab}=0}. \quad (39)$$

It is worth mentioning that, alternatively, the observable parameters σ'_{xx} , z'_{ab} and z' can be found from the background field procedure.

III. ONE-LOOP RENORMALIZATION

A. Perturbative expansions

To define the theory for the perturbative expansions we use the ‘‘square-root’’ parameterization:

$$Q = W + \Lambda \sqrt{1 - W^2}, \quad W = \begin{pmatrix} 0 & w \\ w^\dagger & 0 \end{pmatrix}. \quad (40)$$

The action (30) can be written as the infinite series in the independent fields w and w^\dagger . At short length scales $L \ll \sqrt{\sigma_{xx}/(z_{ab}\Delta_{ab})}$ which we are interested in, the symmetry breaking term \mathcal{S}_{SB} can be omitted. Then the propagators for fields w and w^\dagger can be written in the following form

$$\begin{aligned} & \langle [w_{ab}(\mathbf{q})]_{n_1 n_2}^{\alpha_1 \alpha_2} [w_{cd}^\dagger(-\mathbf{q})]_{n_4 n_3}^{\alpha_4 \alpha_3} \rangle = \frac{4}{\sigma_{xx}} \\ & \times D_q(\omega_{12}) \left[\delta_{n_1 n_3} - \frac{32\pi T \Gamma_{ab}}{\sigma_{xx}} \delta^{\alpha_1 \alpha_2} D_q^{(ab)}(\omega_{12}) \right] \\ & \times \delta_{ab;cd} \delta^{\alpha_1 \alpha_3} \delta^{\alpha_2 \alpha_4} \delta_{n_{12}, n_{34}}, \end{aligned} \quad (41)$$

where $\omega_{12} = \varepsilon_{n_1} - \varepsilon_{n_2} = 2\pi T n_{12} = 2\pi T(n_1 - n_2)$ and

$$\begin{aligned} D_q^{-1}(\omega_n) &= q^2 + \frac{16z\omega_n}{\sigma_{xx}}, \\ [D_q^{(ab)}(\omega_n)]^{-1} &= q^2 + \frac{16(z + \Gamma_{ab})\omega_n}{\sigma_{xx}}. \end{aligned} \quad (42)$$

We use the convention that the Matsubara frequency indices with odd subscripts n_1, n_3, \dots run over non-negative integers whereas those with even subscripts n_2, n_4, \dots run over negative integers.

B. Relation of z_{ab} with z and Γ_{ab}

The dynamical susceptibility $\chi_{ab}(\omega, \mathbf{q})$ which describes the linear response of the system to time-dependent symmetry breaking amplitude Δ_{ab} can be obtained from⁵

$$\chi_{ab}(i\omega_n, \mathbf{q}) = \frac{2z_{ab}}{\pi} - T z_{ab}^2 \langle \text{tr} I_n^\alpha t_{ab} Q(\mathbf{q}) \text{tr} I_{-n}^\alpha t_{ab} Q(-\mathbf{q}) \rangle \quad (43)$$

by the analytic continuation to the real frequencies: $i\omega_n \rightarrow \omega + i0^+$. In the tree level approximation Eq. (43) yields

$$\chi_{ab}(i\omega_n, \mathbf{q}) = \frac{2z_{ab}}{\pi} \left(1 - \frac{16z_{ab}\omega_n}{\sigma_{xx}} D_q^{(ab)}(\omega_n) \right). \quad (44)$$

The action $\mathcal{S}_\sigma + \mathcal{S}_F$ is invariant under the global rotations $Q \rightarrow u Q u^{-1}$ with $u = \sum_{a=0}^1 \sum_{b=0}^3 u_{ab} t_{ab}$. This implies that the quantities corresponding to operators m^{0b} and m^{1b} conserve, i.e., $\chi_{0b}(\omega, \mathbf{q} = 0) = \chi_{1b}(\omega, \mathbf{q} = 0) = 0$. In order to be consistent with this physical requirement, the relations

$$\begin{aligned} z_{ab} &= z + \Gamma_t = z(1 + \gamma_t), \quad a = 0, 1, b = 1, 2, 3, \\ z_{10} &= z + \tilde{\Gamma}_s = z(1 + \tilde{\gamma}_s). \end{aligned} \quad (45)$$

should hold. Therefore, renormalization of the interaction amplitudes $\tilde{\Gamma}_s$ and Γ_t can be easily found from, e.g., renormalized quantities z'_{01} and z'_{10} . However, it is not the case for the interaction amplitude $\Gamma_v = z\gamma_v$. There is no simple relation between Γ_v and

$$z_v = z_{2b} = z_{3b}, \quad b = 0, \dots, 3. \quad (46)$$

Therefore, the physical observables σ'_{xx} , z' , $\tilde{\gamma}'_s$, γ'_t , γ'_v and z'_v completely determines the renormalization of the theory (30) at short length scales $L \ll \sqrt{\sigma_{xx}/z_{ab}\Delta_{ab}}$.

C. One-loop results

Evaluation of the conductance according to Eq. (37) in the one-loop approximation yields

$$\begin{aligned} \sigma'_{xx}(i\omega_n) &= \sigma_{xx} - \frac{128\pi T}{\omega_n \sigma_{xx} \mathbb{D}} \int \frac{d^{\mathbb{D}}\mathbf{p}}{(2\pi)^{\mathbb{D}}} p^2 \sum_{ab} \Gamma_{ab} \sum_{\omega_m > 0} \\ & \times \min\{\omega_m, \omega_n\} D_p(\omega_m + \omega_n) D_p(\omega_m) D_p^{(ab)}(\omega_m). \end{aligned} \quad (47)$$

Performing the analytic continuation to the real frequencies, $i\omega_n \rightarrow \omega + i0^+$, one obtains the DC conductance in the one-loop approximation:

$$\begin{aligned} \sigma'_{xx} &= \sigma_{xx} + \frac{32}{\sigma_{xx} \mathbb{D}} \text{Im} \int \frac{d^{\mathbb{D}}\mathbf{p}}{(2\pi)^{\mathbb{D}}} p^2 \sum_{ab} \Gamma_{ab} \int d\Omega \\ & \times \frac{\partial}{\partial \Omega} \left(\Omega \coth \frac{\Omega}{2T} \right) [D_p^R(\Omega)]^2 D_p^{(ab),R}(\Omega). \end{aligned} \quad (48)$$

Here $D_p^R(\Omega)$ and $D_p^{(ab),R}(\Omega)$ are retarded propagators corresponding to $D_p(\omega_n)$ and $D_p^{(ab)}(\omega_n)$, respectively:

$$\begin{aligned} [D_p^R(\Omega)]^{-1} &= p^2 - (16z/\sigma_{xx}) i\Omega, \\ [D_p^{(ab),R}(\Omega)]^{-1} &= p^2 - (16(z + \Gamma_{ab})/\sigma_{xx}) i\Omega. \end{aligned} \quad (49)$$

We mention that the result (48) can be also obtained with the help of the background field procedure⁵⁰ applied to the action (31)-(32).

In order to compute z' , we have to evaluate the thermodynamic potential Ω . In the one-loop approximation we find

$$\begin{aligned} T^2 \frac{\partial \Omega / T}{\partial T} &= 8N_r T \sum_{\omega_n > 0} \omega_n \left[z + \frac{2}{\sigma_{xx}} \sum_{ab} \int \frac{d^{\mathbb{D}}\mathbf{p}}{(2\pi)^{\mathbb{D}}} \right. \\ & \left. \times \left[(z + \Gamma_{ab}) D_p^{(ab)}(\omega_n) - z D_p(\omega_n) \right] \right]. \end{aligned} \quad (50)$$

Following definition (38), we obtain from Eq. (50)

$$z' = z + \frac{2}{\sigma_{xx}} \sum_{ab} \Gamma_{ab} \int \frac{d^{\mathbb{D}}\mathbf{p}}{(2\pi)^{\mathbb{D}}} D_p(0). \quad (51)$$

Next, we evaluate in the one-loop approximation the generalized susceptibility $\chi_{ab}(i\omega_n, \mathbf{q})$ at $q = 0$ and $\omega_n \rightarrow 0$.

Then, according to Eq. (39), we find

$$z'_{ab} = z_{ab} + \frac{32\pi z_{ab}^2}{\sigma_{xx}^2} \sum_{cd;ef} [\mathcal{C}_{cd;ef}^{ab}]^2 \int \frac{d^{\mathbb{D}}\mathbf{p}}{(2\pi)^{\mathbb{D}}} T \sum_{\omega_m > 0} \times \left[D_p^{(ef)}(\omega_m) D_p^{(cd)}(\omega_m) - D_p^2(\omega_m) \right], \quad (52)$$

where $\mathcal{C}_{cd;ef}^{ab}$ denotes the structural constants of $SU(4)$: $[t_{cd}, t_{ef}] = \sum_{ab} \mathcal{C}_{cd;ef}^{ab} t_{ab}$. Applying Eq. (52) for $(ab) = (10)$ and $(ab) = (01)$, and by virtue of relations (45) we obtain

$$z' + \tilde{\Gamma}'_s = z + \tilde{\Gamma}_s - \frac{2^{10}\pi(z + \tilde{\Gamma}_s)^2}{\sigma_{xx}^2} \int \frac{d^{\mathbb{D}}\mathbf{p}}{(2\pi)^{\mathbb{D}}} T \sum_{\omega_m > 0} \times \left\{ [D_p^{(20)}(\omega_m)]^2 - D_p^2(\omega_m) \right\}, \quad (53)$$

$$z' + \Gamma'_t = z + \Gamma_t - \frac{2^9\pi(z + \Gamma_t)^2}{\sigma_{xx}^2} \int \frac{d^{\mathbb{D}}\mathbf{p}}{(2\pi)^{\mathbb{D}}} T \sum_{\omega_m > 0} \times \left\{ [D_p^{(01)}(\omega_m)]^2 + [D_p^{(20)}(\omega_m)]^2 - 2D_p^2(\omega_m) \right\}. \quad (54)$$

In order to find renormalization of Γ_v , one cannot use the static generalized susceptibility since there exists no simple relation between z_v and Γ_v . We use the the background-field renormalization procedure (see details in Appendix A) and find

$$\Gamma'_{ab} = \Gamma_{ab} - \frac{1}{8\sigma_{xx}} \int \frac{d^{\mathbb{D}}\mathbf{p}}{(2\pi)^{\mathbb{D}}} D_p(0) \sum_{cd;ef} \Gamma_{cd} [\text{sp}(t_{cd} t_{ef} t_{ab})]^2 - \frac{32\pi T}{\sigma_{xx}^2} \sum_{\omega_m > 0} \int \frac{d^{\mathbb{D}}\mathbf{p}}{(2\pi)^{\mathbb{D}}} \sum_{cd;ef} [\mathcal{C}_{cd;ef}^{ab}]^2 \left\{ \Gamma_{ab}^2 D_p^2(\omega_m) - \left[\Gamma_{cd} \Gamma_{ef} + \Gamma_{ab}^2 - 2\Gamma_{ab} \Gamma_{cd} \right] D_p^{(cd)}(\omega_m) D_p^{(ef)}(\omega_m) \right\}. \quad (55)$$

Here symbol sp denotes trace over spin and isospin indices. Using Eq. (55) for $(ab) = (02)$, we obtain

$$\Gamma'_v = \Gamma_v - \frac{2(\Gamma_s - \tilde{\Gamma}_s)}{\sigma_{xx}} \int \frac{d^{\mathbb{D}}\mathbf{p}}{(2\pi)^{\mathbb{D}}} D_p(0) + \frac{2^{10}\pi\Gamma_v^2}{\sigma_{xx}} T \sum_{\omega_m > 0} \int \frac{d^{\mathbb{D}}\mathbf{p}}{(2\pi)^{\mathbb{D}}} D_p^2(\omega_m). \quad (56)$$

It is worthwhile to mention that the results (51), (53) and (54) can be also derived from Eq. (55). Equations (48) (51), (53), (54) and (56) allow us to extract one-loop renormalization of conductance σ_{xx} , parameter z and interaction amplitudes $\tilde{\Gamma}_s$, Γ_t and Γ_v .

D. Renormalization group equations

Applying the minimal subtraction scheme (see, e.g., Ref. 50) to Eqs. (48), (51), (54), (53) and (56), we derive the following one-loop results for the renormalization

group (RG) equations which determine the $T = 0$ behavior of the physical observables with changing the length scale L in $\mathbb{D} = 2$ dimensions:

$$\frac{d\sigma_{xx}}{d\xi} = -\frac{2}{\pi} [1 + f(\tilde{\gamma}_s) + 6f(\gamma_t) + 8f(\gamma_v)], \quad (57)$$

$$\frac{d\tilde{\gamma}_s}{d\xi} = \frac{1 + \tilde{\gamma}_s}{\pi\sigma_{xx}} \left[1 - 6\gamma_t - \tilde{\gamma}_s + 8\gamma_v + 16\gamma_v \frac{\tilde{\gamma}_s - \gamma_v}{1 + \gamma_v} \right], \quad (58)$$

$$\frac{d\gamma_t}{d\xi} = \frac{1 + \gamma_t}{\pi\sigma_{xx}} \left[1 - \tilde{\gamma}_s + 2\gamma_t + 8\gamma_v \frac{\gamma_t - \gamma_v}{1 + \gamma_v} \right], \quad (59)$$

$$\frac{d\gamma_v}{d\xi} = \frac{1}{\pi\sigma_{xx}} \left[1 + \tilde{\gamma}_s + \gamma_v - \gamma_v(6\gamma_t + \tilde{\gamma}_s) + 8\gamma_v^2 \right], \quad (60)$$

$$\frac{d \ln z}{d\xi} = \frac{1}{\pi\sigma_{xx}} \left[\tilde{\gamma}_s + 6\gamma_t + 8\gamma_v - 1 \right]. \quad (61)$$

Here $f(x) = 1 - (1 + x^{-1}) \ln(1 + x)$, $\xi = \ln L/l$ and we omit primes for a brevity. Equations (57)-(60) constitute one of the main results of the present paper and describe the system at the length scales $L \ll \sqrt{\sigma_{xx}/(z_{ab}\Delta_{ab})}$.

It is worthwhile to mention that the right hand side of Eqs. (58) and (59) is not polynomial in the interaction amplitude γ_v . To the best of our knowledge, the one-loop RG equations for interaction amplitudes are quadratic polynomials in all cases studied previously.^{5,13,14,18,38} This fact is deeply related with invariance of the action $\mathcal{S}_\sigma + \mathcal{S}_F$ under the global rotation of the matrix Q with the matrix $\exp(i\hat{\chi})$ (see Sec. IID1). As it follows from Eqs. (36), $\mathcal{S}_\sigma + \mathcal{S}_F$ is invariant under such global rotation with $\chi_{ab} = \chi\delta_{ac}\delta_{bd}$ where $c = 0, 1$ and $d = 1, 2$ or 3 provided $\gamma_t = -1$. The same holds for the global rotation with $\chi_{ab} = \chi\delta_{a1}\delta_{b0}$ if $\tilde{\gamma}_s = -1$. This invariance guarantees that $\gamma_t = -1$ and $\tilde{\gamma}_s = -1$ are fixed points of the RG equations. Therefore, the latter have to be well-defined at $\gamma_t = -1$ and $\tilde{\gamma}_s = -1$. However, for $\gamma_v = -1$ the action $\mathcal{S}_\sigma + \mathcal{S}_F$ is not invariant under the global rotation of the matrix Q with $\chi_{ab} = \chi\delta_{ac}\delta_{bd}$ with $c = 1, 2$ and $d = 0, 1, 2$ or 3 . It is exactly this noninvariance that allows appearance of factors $1/(1 + \gamma_v)$ (diverging at $\gamma_v = -1$) in Eqs. (58) and (59).

The renormalization group equations (57)-(60) possess a rich four-dimensional $(\sigma_{xx}, \tilde{\gamma}_s, \gamma_t, \gamma_v)$ flow diagram. First of all, there is the two-dimensional surface $\gamma_t = \gamma_v = \tilde{\gamma}_s$ which is conserved under RG flow. It corresponds to the case of coinciding quantum wells ($d = 0$). In this case, the RG equations (57)-(61) are completely equivalent to ones for the two-valley electron liquid. However, this two-dimensional surface is unstable: a small initial mismatch (e.g., due to finite d) in the condition $\gamma_t = \gamma_v = \tilde{\gamma}_s$ increases during RG flow. Secondly, the RG flow conserves the two-dimensional surface $\gamma_v = 0$, $\tilde{\gamma}_s = -1$ which is stable. It describes the limit of two separate quantum wells ($d = \infty$). In addition, there are some interesting features of RG flow. For example, there is a two-dimensional surface $\gamma_t = \tilde{\gamma}_s = -1$ which is conserved by RG flow. There is an accidental fixed line $\tilde{\gamma}_s = -1$, $\gamma_v = -1/2$, $\gamma_t = -1/3$. However, these features are not accessible in the double quantum well structure.

Indeed, the initial values of the parameters γ_t , γ_v and

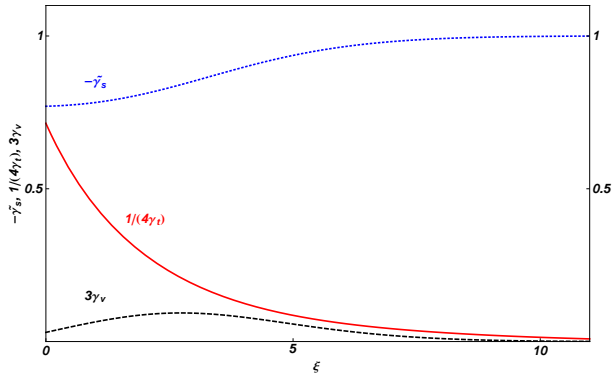


FIG. 3: Dependence of the parameters γ_t , γ_v , $\tilde{\gamma}_s$ on ξ . Initial values are $\tilde{\gamma}_t = 0.35$, $\tilde{\gamma}_v = 0.01$, $\tilde{\gamma}_s = -0.77$, and $\bar{\sigma}_{xx} = 6$.

$\tilde{\gamma}_s$ satisfy

$$\tilde{\gamma}_t \geq \tilde{\gamma}_v \geq 0, \quad \tilde{\gamma}_t \geq \tilde{\gamma}_s. \quad (62)$$

Then, using Eq. (58)-(60) one can prove that under RG flow i) the conditions $\gamma_t \geq \gamma_v \geq 0$ and $\gamma_t \geq \tilde{\gamma}_s$ hold; ii) γ_t always increases. Starting from initial values of the parameters γ_t , γ_v and $\tilde{\gamma}_s$ satisfying Eq. (62) the RG flow develops in such a way that γ_v vanishes, $\tilde{\gamma}_s$ tends to -1 and γ_t increases towards infinity as shown in Fig. 3.

The conductance σ_{xx} demonstrates metallic behavior as in the case of two-valley electron liquid. It increases at large length scales. Depending on the sign of the parameter $K_{ee} = 1 + f(\tilde{\gamma}_s) + 6f(\tilde{\gamma}_t) + 8f(\tilde{\gamma}_v)$, the conductance can develop both monotonic ($K_{ee} < 0$) and non-monotonic behavior ($K_{ee} > 0$) (see Fig. 4). The phase diagram for the parameter K_{ee} is shown in Fig. 5. At $\varkappa/k_F \lesssim 0.4$ the parameter K_{ee} is positive for all values of $\varkappa d$. With increasing \varkappa/k_F a domain of negative values of K_{ee} develops at small values of $\varkappa d$.

The conductance σ'_{xx} defined in Eq. (37) and renormalized in accordance with Eq. (57) is the total conductance of double quantum well structure. In general, one can write $\sigma'_{xx} = \sigma'_{11} + \sigma'_{22} + \sigma'_{12} + \sigma'_{21}$, where σ'_{11} and σ'_{22} are the intrawell conductances of left and right quantum wells respectively, and σ'_{12} and σ'_{21} denote the transconductances responsible for a drag effect. At the balance, symmetry yields that $\sigma'_{11} = \sigma'_{22}$ and $\sigma'_{12} = \sigma'_{21}$.

Although in experiments of Refs. [31,32] only the total conductivity σ'_{xx} has been measured, such double quantum well heterostructures with correlated disorder at the balance allow for experimental study of transconductance contrary to the two-valley electron system in Si-MOSFET. It was shown³⁶ that in the presence of electron-electron interaction one-loop contribution in the particle-hole channel (only “diffusons”) to the DC transconductance σ'_{12} vanishes. As a result, the one-loop contribution to the DC transconductance is entirely determined by the particle-particle channel (“Cooperons”). However, in Ref. [36] only the interwell interactions (U_{12}^{scr}) were taken into account. As shown in Appendix B, an accurate treatment of both interwell (U_{12}^{scr}) and intrawell

(U_{11}^{scr}) interactions (i.e. taking into account all interaction couplings Γ_s , $\tilde{\Gamma}_s$, Γ_t , and Γ_v) does not change the conclusion of Ref. [36]: the particle-hole (“diffuson”) contribution to the DC transconductance σ'_{12} vanishes in the one-loop approximation.

IV. DEPHASING RATE

The presence of the right well changes the properties of electrons in the left well. One of the important quantities characterizing interacting electrons in a random potential is the dephasing rate. Its dependence on temperature determines the behavior of the weak-localization correction to the conductance. In this section, we investigate how the presence of the right well changes the dephasing rate of electrons in the left well compared to the case when the right well is empty.

A. Contribution from the interaction in the singlet channel

We start from the case of the interaction in the singlet channel only. According to Eq. (21), electrons in the right well screen interaction between electrons in the left well and vice versa. The dephasing rate of electrons in the left well due to the presence of electrons in the right well can be found from the following expression which generalizes standard on:^{33,51}

$$\frac{1}{\tau_\varphi} = - \int_{\tau_\varphi^{-1}} \frac{d\omega}{\pi} \int \frac{d^2q}{(2\pi)^2} \frac{\text{Im} U_{11}^{\text{scr}}(\mathbf{q}, \omega)}{\sinh(\omega/T)} \frac{D_1 q^2}{D_1^2 q^4 + \omega^2}. \quad (63)$$

Expression for the dephasing rate of electrons in the right well can be obtained from Eq. (63) by substitution of U_{22} and D_2 for U_{11} and D_1 , respectively. At the balance which we are interested in, the dephasing rates in the left and right wells are the same. Under the following assumption $d, \varkappa^{-1} \ll L_T = \sqrt{D/T}$, we find

$$\frac{1}{\tau_\varphi} = \mathcal{A}_s \frac{T}{8\pi\nu D} \ln T\tau_\varphi \quad (64)$$

where \mathcal{A}_s is the function of the parameter $\varkappa d$:

$$\mathcal{A}_s = \frac{1}{2} \left[1 + \frac{(\varkappa d)^2}{(1 + \varkappa d)(2 + \varkappa d)} \right]. \quad (65)$$

We mention that in the absence of electrons in the right well (formally this case corresponds to the limit $d \rightarrow \infty$) the dephasing rate is maximal: $\mathcal{A}_s = 1$. Equation (65) was used for analysis of the experimental data in Ref. [31].

B. Contribution from the interaction in the multiplet channels

In general case, one has to take into account contributions to the dephasing rate from the interaction in mul-

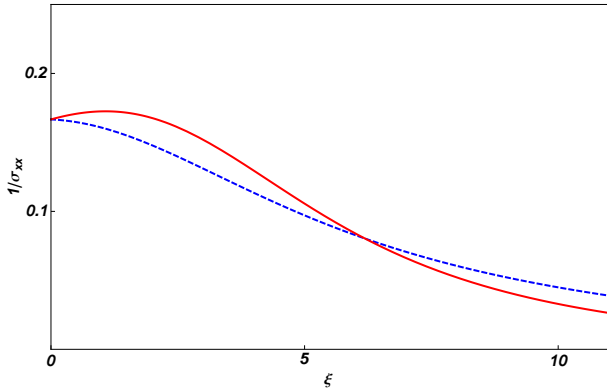


FIG. 4: Dependence of the inverse conductance $1/\sigma_{xx}$ on ξ . Solid (red) curve is plotted with initial values $\tilde{\gamma}_t = 0.35$, $\tilde{\gamma}_v = 0.01$, $\tilde{\gamma}_s = -0.77$, and $\tilde{\sigma}_{xx} = 6$. Dashed (blue) curve corresponds to $\tilde{\gamma}_t = 0.198$, $\tilde{\gamma}_v = 0.135$, $\tilde{\gamma}_s = 0.57$, and $\tilde{\sigma}_{xx} = 6$.

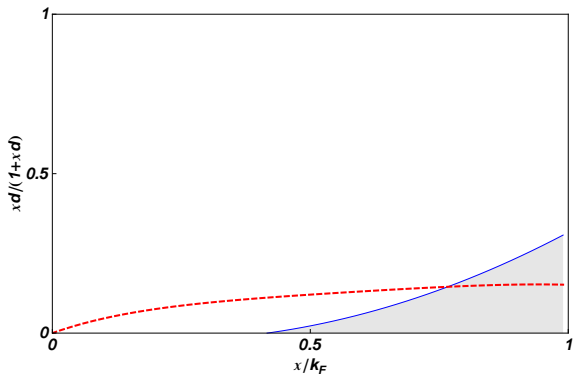


FIG. 5: The phase diagram for the parameter $K_{ee} = 1 + f(\tilde{\gamma}_s) + 6f(\tilde{\gamma}_t) + 8f(\tilde{\gamma}_v)$. It vanishes on the solid (blue) line. K_{ee} is negative in the filled region below the solid (blue) curve and is positive above. Dashed (red) line indicates $\tilde{F}_s = 0$.

triplet channels.³⁴ We restrict ourselves to the case of the balance. Generalizing the well-known result³³ for the single well we can write the dephasing rate in the left well as

$$\frac{1}{\tau_\varphi} = -\frac{2}{\sigma_{xx}} \int_{\tau_\varphi^{-1}} d\omega \int \frac{d^2q}{(2\pi)^2} \frac{\text{Re} D_q^R(\omega)}{\sinh(\omega/T)} \sum_{ab} \text{Im} \mathcal{U}^{(ab)}(q, \omega) \quad (66)$$

where

$$\mathcal{U}^{(ab)}(q, \omega) = \frac{\Gamma_{ab}}{z} D_q^{(ab),R}(\omega) [D_q^R(\omega)]^{-1}. \quad (67)$$

Performing integration over momentum and frequency, we find

$$\frac{1}{\tau_\varphi} = \mathcal{A} \frac{T}{2\sigma_{xx}} \ln T\tau_\varphi \quad (68)$$

with

$$\mathcal{A} = \frac{1}{2} \left[1 + \frac{\tilde{\gamma}_s^2}{2 + \tilde{\gamma}_s} + 6 \frac{\tilde{\gamma}_t^2}{2 + \tilde{\gamma}_t} + 8 \frac{\tilde{\gamma}_v^2}{2 + \tilde{\gamma}_v} \right]. \quad (69)$$

In the absence of interaction in the multiplet channels, i.e., for $F_t = F_v = 0$ and $\tilde{\gamma}_s = -\varkappa d/(1 + \varkappa d)$, this result transforms into Eq. (64). We mention that the interaction parameters $\tilde{\gamma}_s$, $\tilde{\gamma}_t$ and $\tilde{\gamma}_v$ as well as conductance σ_{xx} should be taken at the length scale $L_T = \sqrt{\sigma_{xx}/zT}$.

It is worthwhile to compare Eq. (68) with the result for the dephasing rate in the absence of electrons in the right well.³³ Taking the limit $d \rightarrow \infty$, i.e., setting $\tilde{\gamma}_s = -1$, $\tilde{\gamma}_v = 0$, and $\tilde{\gamma}_t = \gamma_{t,0}$, we obtain

$$\mathcal{A} \rightarrow \mathcal{A}_0 = \left[1 + \frac{3\gamma_{t,0}^2}{2 + \gamma_{t,0}} \right] \quad (70)$$

where initial value of $\gamma_{t,0}$ is $\tilde{\gamma}_{t,0} = -F_t^0/(1 + F_t^0)$.

V. COMPARISON WITH THE EXPERIMENT

Recently, the interference³¹ and interaction³² corrections to the conductivity of the gated double quantum well $\text{Al}_x\text{Ga}_{1-x}\text{As}/\text{GaAs}/\text{Al}_x\text{Ga}_{1-x}\text{As}$ heterostructures have been studied. Two heterostructures, 3243 and 3154, distinguishing by the doping level have been investigated. From analysis of positive magnetoconductivity the dephasing rate has been extracted. By tuning the gate voltage, the electron concentration in the right quantum well were controlled in the experiment.

We consider two characteristic cases: I) electron concentrations and mobilities (\mathcal{M}) of both quantum wells are equal: $n_1 = n_2 = n$ and $\mathcal{M}_1 = \mathcal{M}_2 = \mathcal{M}$; II) the left quantum well has electron concentration $n_1 = n$ and mobility $\mathcal{M}_1 = \mathcal{M}$ whereas the right quantum well has electron concentration $n_2 = 0$. The electron concentration n has been high such that the conductance $\tilde{\sigma}_{xx}$ was about 80. Therefore, physics described by RG equations (57)-(61) was not observed. The main unexpected findings of Refs. [31,32] were as follows. Dephasing rates (coefficient \mathcal{A}) and interaction correction (parameter K_{ee}) extracted in cases I) and II) were practically the same. At first glance, it is counterintuitive since there are 15 multiplets in the case I) and only 3 in the case II).

After Refs. [31,32] we summarize the experimental values of relevant parameters in Table I. The theoretical estimates for the interaction parameters in cases I) and II) are presented in Table II. As one can see, in the experimentally studied case of $\varkappa d = 3.6$ the interaction parameter F_v is negligible, F_t and F_t^0 coincide with each other and \tilde{F}_s is equal approximately to $\varkappa d$. The comparison between theoretical estimates for K_{ee} , \mathcal{A} , $K_{ee,0}$ and \mathcal{A}_0 with experimental data (wherever it is possible) is summarized in Table III. Our theoretical estimates are in good quantitative agreement with the experimental ones. Our results explain why the interaction corrections and dephasing rates in cases I) and II) were found to be practically the same in the experiments.^{31,32} Since the parameter $K_{ee,0}$ is positive for $\varkappa/k_F \lesssim 1$ a drastic effect in the interaction correction could be seen by tuning the gate voltage from case I) to case II) in double quantum

TABLE I: Parameters for samples studied in Refs. [31,32]

sample	#3154	#3243
$n, 10^{11} \text{ cm}^{-2}$	4.5	7.5
$k_F, 10^6 \text{ cm}^{-1}$	1.7	2.2
$\varkappa, 10^6 \text{ cm}^{-1}$	2	2
$d, 10^{-6} \text{ cm}$	1.8	1.8
$\varkappa d$	3.6	3.6
$k_F d$	3.06	3.95
\varkappa/k_F	1.18	0.91

TABLE II: Theoretical estimates of interaction parameters.

sample	#3154	#3243
\tilde{F}_s	3.34	3.37
F_t	-0.26	-0.23
F_v	-0.009	-0.007
$\tilde{\gamma}_s$	-0.77	-0.77
$\tilde{\gamma}_t$	0.35	0.30
$\tilde{\gamma}_v$	0.009	0.007
F_t^0	-0.26	-0.23
$\tilde{\gamma}_{t,0}$	0.35	0.30

well structures with $\varkappa d \lesssim 1$ for which one can expect $K_{ee} < 0$ (see Fig. 5).

As mentioned in the Introduction, our theory is valid at temperatures $T \gg \Delta_{SAS}, \Delta_s, 1/\tau_{+-}$. In the experiments of Refs. [31,32] the Zeeman splitting (at relevant magnetic field which was used in order to extract interaction correction) and Δ_{SAS} were estimated as $\Delta_s \lesssim 0.2K$ and $\Delta_{SAS} \lesssim 1K$. A small asymmetry in the impurity distribution along z axis presented in the double quantum well heterostructures used in Refs. [31,32] leads to appearance of scattering rate between symmetric and antisymmetric states. The corresponding scattering rate ($1/\tau_{+-}$) can be estimated from temperature and magnetic field dependence of weak-localization (interference) correction to conductivity.

TABLE III: Comparison of theoretical estimates and experimental findings [$K_{ee,0} = 1 + 3f(\tilde{\gamma}_{t,0})$, $K_{ee} = 1 + f(\tilde{\gamma}_s) + 6f(\tilde{\gamma}_t) + 8f(\tilde{\gamma}_v)$].

	Theory		Experiment	
	#3154	#3243	#3154	#3243
K_{ee}	0.59	0.72	0.50 ± 0.05	0.57 ± 0.05
$K_{ee,0}$	0.52	0.59	0.53 ± 0.05	0.60 ± 0.05
\mathcal{A}	0.89	0.86		
\mathcal{A}_0	1.15	1.12		
$\mathcal{A}/\mathcal{A}_0$	0.77	0.77	1.00 ± 0.05	1.00 ± 0.05

As known,^{33,42,43} in the absence of scattering between symmetric and antisymmetric states neither Δ_s nor Δ_{SAS} does not influence the weak-localization contribution. In the absence of magnetic field, the weak localization correction to the conductance in both asymptotic cases $\Delta_{SAS} \ll 1/\tau_{+-}$ and $\Delta_{SAS} \gg 1/\tau_{+-}$ can be written as

$$\delta\sigma_{xx}^{WL} = \frac{1}{\pi} \ln \left[\frac{\tau_{\text{tr}}^2}{\tau_\varphi} \left(\frac{1}{\tau_\varphi} + \frac{1}{\tau_{12}} \right) \right] \quad (71)$$

where $1/\tau_{12} \sim \min\{\Delta_{SAS}^2\tau_{+-}, 1/\tau_{+-}\}$. The temperature dependence of the weak-localization correction (71) smoothly interpolates between the result known for a two-valley system at high temperatures ($1/\tau_\varphi \gg 1/\tau_{12}$) and the single-valley result at low temperatures ($1/\tau_\varphi \ll 1/\tau_{12}$). In experiments [31] the characteristic time τ_{12} was estimated from the suppression of weak-localization correction due to perpendicular magnetic field as $1/\tau_{12} \lesssim 0.1K$. Together with the estimate $\Delta_{SAS} \lesssim 1K$ it implies that $1/\tau_{+-} \sim 1/\tau_{12} \lesssim 0.1K$. Therefore our theory is applicable at temperatures $T \gtrsim 1K$. It is this temperature range that was studied experimentally in Refs. [31,32].

VI. CONCLUSIONS

To summarize, we have developed the theory of the disordered electron liquid in a double well quantum heterostructure with equal electron concentrations. We have identified all relevant interaction parameters and found their dependence on the distance between quantum wells. To describe the system at low temperatures, we have derived the interacting non-linear sigma model and studied it renormalization in the one-loop approximation. We have obtained the renormalization group equations describing the length scale dependence of the conductance and interaction parameters. We have found that upon the renormalization the system flows towards the fixed point corresponding to two separate quantum wells. The RG equations predict the metallic behavior of the conductance. We have evaluated the dephasing rate of electrons due to the presence of electron-electron interaction. This expression takes into account screening of electron-electron interaction within one quantum well by electrons from the other quantum well.

We did not consider contributions to the one-loop RG equations from the particle-particle (“Cooper”) channel. The interaction effects related to the Cooper channel are governed by the corresponding interaction amplitude which is always small for 2D electron systems with Coulomb repulsion, so that one can neglect it.⁵ As for the interference contribution to conductance, for $1/\tau_\varphi \gg 1/\tau_{12}$, it can be taken into account by the substitution of $1+2$ for 1 in the square brackets of Eq. (57). This does not change qualitative behavior of the interaction amplitudes $\tilde{\gamma}_s, \gamma_t$ and γ_v discussed above. However, the interference contribution makes behavior of the conductance always non-monotonous.

We performed detailed comparison between our theory and experimental data.^{31,32} We explained main experimental results and found good quantitative agreement. It would be an experimental challenge to construct the double quantum well heterostructure with $\kappa d \lesssim 1$. Then, according to our predictions, one can expect a change from non-monotonous to monotonous behavior in conductance in the presence of small perpendicular magnetic field (to suppress interference contribution) when the right well is depopulated by tuning the gate voltage. It would be also interesting to experimentally study the Coulomb drag effect in such heterostructures with correlated disorder.

Finally it would be worthwhile to extend our analysis to temperatures less than the symmetry breaking energy scales Δ_{SAS} , Δ_s and $1/\tau_{+-}$. At such low temperatures one may expect different behavior of transport in double quantum well structures as compared to two-valley electron systems studied recently.^{13,14,18}

Acknowledgments

The authors thank A. Ioselevich and A. Yashenkin for useful discussions, and are grateful to G. Minkov, A. Germanenko and A. Sherstobitov for detailed description of their experimental data prior to publication. The research was funded in part by the Council for Grant of the President of Russian Federation (Grant No. MK-125.2009.2), RFBR (Grant Nos 09-02-12206 and 09-02-00247-a), RAS Programs ‘‘Quantum Physics of Condensed Matter’’ and ‘‘Fundamentals of nanotechnology and nanomaterials’’, the Russian Ministry of Education and Science under contract No. P926, by the Center for Functional Nanostructures of the Deutsche Forschungsgemeinschaft, by the DFG-RFBR cooperation grant, and by the EUROHORCS/ESF EURYI Awards scheme. The work by K.S.T. was supported by Dynasty Foundation. I.S.B. is grateful to the Institute of Nanotechnology and Institute of Condensed Matter Theory at Karlsruhe Institute of Technology for hospitality.

Appendix A: Background field renormalization of the Finkelstein term \mathcal{S}_F

In this appendix we present details of the derivation of Eq. (55) with the help of the background field renormalization. Let us separate the matrix field Q into the ‘‘fast’’ (Q) and ‘‘slow’’ ($Q_0 = T_0^{-1}\Lambda T_0$) modes as

$$Q \rightarrow T_0^{-1}QT_0. \quad (\text{A1})$$

The effective action for the Q_0 fields is given by

$$\exp \mathcal{S}_{\text{eff}}[Q_0] = \int \mathcal{D}[Q] \exp \mathcal{S}[T_0^{-1}QT_0] \quad (\text{A2})$$

Since we are interesting in the renormalization of the interaction parameters Γ_{ab} only, we insert the spatial independent background field T_0 in the action (32). The

result can be written as follows

$$\begin{aligned} \mathcal{S}_F[T_0^{-1}QT_0] &= \mathcal{S}_F[Q_0] + \mathcal{S}_F[Q] + O_t^{(1),1} + O_t^{(1),2} \\ &\quad + O_t^{(2),1} + O_t^{(2),2} + Q_\eta, \end{aligned} \quad (\text{A3})$$

where

$$\begin{aligned} O_t^{(1),1} &= -\frac{\pi T}{2} \int d\mathbf{r} \sum_{\alpha n; ab} \Gamma_{ab} \text{tr} I_n^\alpha t_{ab} \delta Q \text{tr} I_{-n}^\alpha t_{ab} Q_0, \\ O_t^{(1),2} &= -\frac{\pi T}{2} \int d\mathbf{r} \sum_{\alpha n; ab} \Gamma_{ab} \text{tr} I_n^\alpha t_{ab} \delta Q \text{tr} A_{-n; ab}^\alpha \delta Q, \\ O_t^{(2),1} &= -\frac{\pi T}{2} \int d\mathbf{r} \sum_{\alpha n; ab} \Gamma_{ab} \text{tr} I_n^\alpha t_{ab} Q_0 \text{tr} A_{-n; ab}^\alpha \delta Q, \\ O_t^{(2),2} &= -\frac{\pi T}{4} \int d\mathbf{r} \sum_{\alpha n; ab} \Gamma_{ab} \text{tr} A_{n; ab}^\alpha \delta Q \text{tr} A_{-n; ab}^\alpha \delta Q, \\ O_\eta &= 4\pi T z \int d\mathbf{r} \text{tr} A_\eta \delta Q. \end{aligned} \quad (\text{A4})$$

Here we introduce $\delta Q = Q - \Lambda$ and

$$A_\eta = T_0[\eta, T_0^{-1}], \quad A_{n; ab}^\alpha = T_0[I_n^\alpha t_{ab}, T_0^{-1}]. \quad (\text{A5})$$

The effective action $\mathcal{S}_{\text{eff}}[Q_0]$ can be obtained by expansion of $\mathcal{S}[T_0^{-1}QT_0]$ to the second order in A_η and $A_{n; ab}^\alpha$.⁸ Then, we find

$$\begin{aligned} \mathcal{S}_{\text{eff}}[Q_0] - \mathcal{S}_F[Q_0] &= \langle O_t^{(2),1} \rangle + \langle O_t^{(2),2} \rangle + \frac{1}{2} \langle [O_t^{(1),1}]^2 \rangle \\ &\quad + \frac{1}{2} \langle O_t^{(1),1} O_t^{(1),2} \rangle + \frac{1}{2} \langle [O_t^{(1),2}]^2 \rangle + \langle O_\eta \rangle, \end{aligned} \quad (\text{A6})$$

where the average $\langle \dots \rangle$ is with respect to action (31)-(32) and we omit terms which do not involve infrared divergencies. In general, each term in the right hand side of Eq. (A6) produce contributions which cannot be expressed in terms of Q_0 only. However, all such contributions cancel in the total expression (A6). Therefore, we will not list them below. Expanding δQ in series of W according to Eq. (40) and performing averaging with the help of Eq. (41), we obtain

$$\begin{aligned} \mathcal{S}_{\text{eff}}[Q_0] &= -\frac{\pi T}{4} \int d\mathbf{r} \sum_{\alpha n; ab} \Gamma'_{ab} \text{tr} I_n^\alpha t_{ab} Q \text{tr} I_{-n}^\alpha t_{ab} Q \\ &\quad + 4\pi T z' \int d\mathbf{r} \text{tr} \eta Q \end{aligned} \quad (\text{A7})$$

where

$$\begin{aligned} \Gamma'_{ab} &= \Gamma_{ab} + \delta\Gamma_{ab}^{(2),1} + \delta\Gamma_{ab}^{(2),2} + \delta\Gamma_{ab}^{(1),1;1} + \delta\Gamma_{ab}^{(1),1;2} \\ &\quad + \delta\Gamma_{ab}^{(1),2;2} + \delta\Gamma_{ab}^\eta \end{aligned} \quad (\text{A8})$$

and similar for z' . Here the contributions to Γ'_{ab} from each term in the right hand side of Eq. (A6) are given as follows

$$\begin{aligned} \langle O_t^{(2),1} \rangle &\rightarrow \delta\Gamma_{ab}^{(2),1} = \frac{32\pi T}{\sigma_{xx}^2} \sum_{cd; ef} [C_{cd; ef}^{ab}]^2 \Gamma_{cd} \Gamma_{ef} \\ &\quad \times \int \frac{d^2 \mathbf{p}}{(2\pi)^2} \sum_{\omega_m > 0} D D_p^{(cd)}(\omega_m), \end{aligned} \quad (\text{A9})$$

$$\begin{aligned} \langle O_t^{(2),2} \rangle &\rightarrow \delta\Gamma_{ab}^{(2),2} = -\frac{1}{8\sigma_{xx}} \sum_{cd;ef} [\text{sp}(t_{cd}t_{ef}t_{ab})]^2 \Gamma_{cd} \\ &\times \int \frac{d^2\mathbf{p}}{(2\pi)^2} D_p(0), \end{aligned} \quad (\text{A10})$$

$$\begin{aligned} \frac{1}{2} \langle [O_t^{(1),1}]^2 \rangle &\rightarrow \delta\Gamma_{ab}^{(1),1;1} = \frac{32\pi T}{\sigma_{xx}^2} \sum_{cd;ef} [\Gamma_{ab} \mathcal{C}_{cd;ef}^{ab}]^2 \sum_{\omega_m > 0} \\ &\times \int \frac{d^2\mathbf{p}}{(2\pi)^2} [D^{(cd)} D_p^{(ef)}(\omega_m) - D_p^2(\omega_m)], \end{aligned} \quad (\text{A11})$$

$$\begin{aligned} \langle O_t^{(1),1} O_t^{(1),2} \rangle &\rightarrow \delta\Gamma_{ab}^{(1),1;2} = -\frac{64\pi T}{\sigma_{xx}^2} \sum_{cd;ef} [\mathcal{C}_{cd;ef}^{ab}]^2 \Gamma_{ab} \Gamma_{cd} \\ &\times \int \frac{d^2\mathbf{p}}{(2\pi)^2} \sum_{\omega_m > 0} D^{(ab)} D_p^{(ef)}(\omega_m), \end{aligned} \quad (\text{A12})$$

$$\begin{aligned} \frac{1}{2} \langle [O_t^{(1),2}]^2 \rangle &\rightarrow \delta\Gamma_{ab}^{(1),2;2} = \frac{32\pi T}{\sigma_{xx}^2} \sum_{cd;ef} [\Gamma_{ef} \mathcal{C}_{cd;ef}^{ab}]^2 \sum_{\omega_m > 0} \\ &\times \int \frac{d^2\mathbf{p}}{(2\pi)^2} [D^{(cd)} D_p^{(ef)}(\omega_m) - DD_p^{(cd)}(\omega_m)], \end{aligned} \quad (\text{A13})$$

and

$$\langle O_\eta \rangle \rightarrow \delta\Gamma_{ab}^\eta = 0. \quad (\text{A14})$$

Combing contributions (A8)-(A14) we obtain Eq. (55).

The only non-zero contributions to renormalization of z are

$$\begin{aligned} \frac{1}{2} \langle [O_t^{(1),2}]^2 \rangle &\rightarrow \delta z^{(1),2;2} = \frac{64\pi T}{\sigma_{xx}^2} \sum_{cd} \Gamma_{cd} \sum_{\omega_m > 0} \\ &\times \int \frac{d^2\mathbf{p}}{(2\pi)^2} [DD_p(\omega_m) - D^{(cd)} D_p^{(cd)}(\omega_m)] \end{aligned} \quad (\text{A15})$$

and

$$\begin{aligned} \langle O_\eta \rangle &\rightarrow \delta z^\eta = -\frac{64\pi T}{\sigma_{xx}^2} \sum_{cd} \Gamma_{cd} \int \frac{d^2\mathbf{p}}{(2\pi)^2} \\ &\times \sum_{\omega_m > 0} DD_p^{(cd)}(\omega_m). \end{aligned} \quad (\text{A16})$$

In total, Eqs. (A15) and (A16) give

$$z' = z + \frac{64\pi T}{\sigma_{xx}^2} \sum_{cd} \Gamma_{cd} \int \frac{d^2\mathbf{p}}{(2\pi)^2} \sum_{\omega_m > 0} D_p^2(\omega_m). \quad (\text{A17})$$

It coincides with Eq. (51).

Appendix B: Evaluation of DC transconductance σ'_{12}

In this appendix we present calculations of the DC transconductance in the one-loop approximation. Similarly to the total conductance, the transconductance can

be obtained from

$$\begin{aligned} \sigma'_{12}(i\omega_n) &= -\frac{\sigma_{xx}}{16n} \langle \text{tr}[I_n^\alpha t_-, Q][I_{-n}^\alpha t_+, Q] \rangle + \frac{\sigma_{xx}^2}{128n} \int d\mathbf{r}' \\ &\times \langle \langle \text{tr} I_n^\alpha t_- Q(\mathbf{r}) \nabla Q(\mathbf{r}) \text{tr} I_{-n}^\alpha t_+ Q(\mathbf{r}') \nabla Q(\mathbf{r}') \rangle \rangle \end{aligned} \quad (\text{B1})$$

after the analytic continuation to the real frequencies: $i\omega_n \rightarrow \omega + i0^+$ at $\omega \rightarrow 0$. Here matrices $t_\pm = (t_{00} \pm t_{30})/2$. Evaluation of the transconductance according to Eq. (B1) in the one-loop approximation yields

$$\begin{aligned} \sigma'_{12}(i\omega_n) &= \frac{32\pi T}{\sigma_{xx}\omega_n} \sum_{ab} \Gamma_{ab} \text{sp}[t_- t_{ab} t_+ t_{ab} - t_- t_+] \sum_{\omega_m > 0} \\ &\times \omega_m \int \frac{d^2\mathbf{p}}{(2\pi)^2} DD_p^{(ab)}(\omega_{m+n}) \\ &- \frac{8\pi T}{\sigma_{xx}\omega_n} \int \frac{d^2\mathbf{p}}{(2\pi)^2} p^2 \sum_{ab;cd} \text{sp}[t_- t_{ab} t_{cd}] \sum_{\omega_m > 0} \\ &\times \left\{ \text{sp}(t_+[t_{ab}, t_{cd}]) \omega_m [\Gamma_{ab} D_p(\omega_{m+n}) DD_p^{(ab)}(\omega_m) \right. \\ &+ \Gamma_{cd} D_p^{(ab)}(\omega_m) DD_p^{(cd)}(\omega_{m+n})] - \text{sp}[t_+ t_{ab} t_{cd}] \\ &\left. \times \Gamma_{ab} \min\{\omega_m, \omega_n\} D_p(\omega_{m+n}) DD_p^{(ab)}(\omega_m) \right\}, \end{aligned} \quad (\text{B2})$$

where $DD_p^{(ab)}(\omega_m) \equiv D_p(\omega_m) D_p^{(ab)}(\omega_m)$. Evaluating the traces we find

$$\begin{aligned} \sigma'_{12}(i\omega_n) &= \frac{2^9 \pi T \Gamma_v}{\sigma_{xx}\omega_n} \int \frac{d^2\mathbf{p}}{(2\pi)^2} \sum_{\omega_m > 0} \left\{ \omega_m [DD_p^{(20)}(\omega_{m+n}) \right. \\ &- p^2 (D_p(\omega_m) + D_p^{(20)}(\omega_{m+n})) D_p(\omega_{m+n}) D_p^{(20)}(\omega_m)] \\ &\left. + \min\{\omega_m, \omega_n\} p^2 D_p(\omega_{m+n}) DD_p^{(20)}(\omega_m) \right\}. \end{aligned} \quad (\text{B3})$$

Performing the analytic continuation to the real frequencies, $i\omega_n \rightarrow \omega + i0^+$, one obtains the DC transconductance in the one-loop approximation:

$$\begin{aligned} \sigma'_{12} &= -\frac{2^7 \Gamma_v}{\sigma_{xx}} \text{Im} \int \frac{d^2\mathbf{p}}{(2\pi)^2} \int d\Omega \left\{ \frac{\partial}{\partial \Omega} \left(\Omega \coth \frac{\Omega}{2T} \right) \right. \\ &\times [DD_p^{(20),R}(\Omega) - p^2 D^2 D_p^{(20),R}(\Omega)] + p^2 \Omega \coth \frac{\Omega}{2T} \\ &\left. \times D_p^{(20),R}(\Omega) \frac{\partial}{\partial \Omega} \left[\frac{1}{2} D_p^2(\Omega) + DD_p^{(20),R}(\Omega) \right] \right\}, \end{aligned} \quad (\text{B4})$$

where $DD_p^{(ab),R}(\Omega) \equiv D_p^R(\Omega) D_p^{(ab),R}(\Omega)$. Next, Eq. (B4) can be simplified as

$$\begin{aligned} \sigma'_{12} &= \frac{2^{11} \Gamma_v}{\sigma_{xx}^2} \text{Re} \int d\Omega \Omega \coth \frac{\Omega}{2T} \\ &\times \int \frac{d^2\mathbf{p}}{(2\pi)^2} p^2 DD_p^{(20),R}(\Omega) \\ &\times \left\{ z [D_p^R(\Omega)]^2 - (z + \Gamma_v) [D_p^{(20),R}(\Omega)]^2 \right\} \end{aligned} \quad (\text{B5})$$

One can check that due to integration over momentum p the DC transconductance vanishes at arbitrary temper-

ature, $\sigma'_{12} = 0$.

-
- ¹ T. Ando, A.B. Fowler, and F. Stern, *Rev. Mod. Phys.* **54**, 437 (1982).
- ² S.V. Kravchenko, G.V. Kravchenko, J.E. Furneaux, V.M. Pudalov, M. D'Iorio, *Phys. Rev. B* **50**, 8039 (1994).
- ³ S. V. Kravchenko, W.E. Mason, G.E. Bowker, J. E. Furneaux, V.M. Pudalov, and M. D'Iorio, *Phys. Rev. B* **51** 7038 (1995).
- ⁴ E. Abrahams, S. V. Kravchenko, and M. P. Sarachik, *Rev. Mod. Phys.* **73**, 251 (2001); S. V. Kravchenko, and M. P. Sarachik, *Rep. Prog. Phys.* **67**, 1 (2004).
- ⁵ A.M. Finkelstein, *Pis'ma v Zh. Éksp. Teor. Fiz.* **37**, 436 (1983) [*JETP Lett.* **37**, 517 (1983)]; *Zh. Éksp. Teor. Fiz.* **84**, 168 (1983) [*Sov. Phys. JETP* **53**, 97 (1983)]; *Zh. Éksp. Teor. Fiz.* **86**, 367 (1984) [*Sov. Phys. JETP* **59**, 212 (1984)]; *Z. Phys. B* **56**, 189 (1984). For review, see A.M. Finkelstein, *Electron liquid in disordered conductors*, vol. 14 of Soviet Scientific Reviews, ed. by I.M. Khalatnikov (Harwood Academic Publishers, London, 1990); in *50 years of Anderson localization*, ed. by E. Abrahams (World Scientific, 2010), p. 385; *Int. J. Mod. Phys. B* **24**, 1855 (2010)
- ⁶ C. Castellani, C. Di Castro, P.A. Lee, and M. Ma, *Phys. Rev. B* **30**, 527 (1984).
- ⁷ A. Punnoose and A.M. Finkelstein, *Science* **310**, 289 (2005).
- ⁸ M.A. Baranov, A.M.M. Pruisken, and B. Škorić, *Phys. Rev. B* **60**, 16821 (1999).
- ⁹ M. A. Baranov, I. S. Burmistrov, and A. M. M. Pruisken, *Phys. Rev. B* **66**, 075317 (2002).
- ¹⁰ D. Simonian, S. V. Kravchenko, M. P. Sarachik, and V. M. Pudalov, *Phys. Rev. Lett.* **79**, 2304 (1997).
- ¹¹ S.A. Vitkalov, K. James, B.N. Narozhny, M.P. Sarachik, and T.M. Klapwijk, *Phys. Rev. B* **67**, 113310 (2003).
- ¹² V.M. Pudalov, M.E. Gershenson, H. Kojima, G. Brunthaler, A. Prinz, and G. Bauer, *Phys. Rev. Lett.* **91**, 126403 (2003).
- ¹³ I.S. Burmistrov and N.M. Chitchev, *Phys. Rev. B* **77**, 195319 (2008).
- ¹⁴ A. Punnoose, *Phys. Rev. B* **81**, 035306 (2010); *ibid* **82**, 115310 (2010).
- ¹⁵ A. Punnoose, and A.M. Finkelstein, *Phys. Rev. Lett.* **88**, 016802 (2001).
- ¹⁶ D.A. Knyazev, O.E. Omel'yanovskii, V.M. Pudalov, and I.S. Burmistrov, *JETP Lett.* **84**, 662 (2006).
- ¹⁷ S. Anissimova, S. V. Kravchenko, A. Punnoose, A. M. Finkelstein, and T. M. Klapwijk, *Nature Phys.* **3**, 707 (2007).
- ¹⁸ A. Punnoose, A. M. Finkelstein, A. Mokashi, S. V. Kravchenko, *Phys. Rev. B* **82**, 201308(R) (2010).
- ¹⁹ D.A. Knyazev, O.E. Omel'yanovskii, V.M. Pudalov, and I.S. Burmistrov, *Phys. Rev. Lett.* **100**, 046405 (2008).
- ²⁰ A. Yu. Kuntsevich, N. N. Klimov, S. A. Tarasenko, N. S. Averkiev, V. M. Pudalov, H. Kojima, M. E. Gershenson, *Phys. Rev. B* **75**, 195330 (2007).
- ²¹ N.N. Klimov, D.A. Knyazev, O.E. Omel'yanovskii, V.M. Pudalov, H. Kojima, and M.E. Gershenson, *Phys. Rev. B* **78**, 195308 (2008).
- ²² M. Shayegan, E.P. De Poortere, O. Gunawan, Y.P. Shkolnikov, E. Tutuc, and K. Vakili, *Phys. Stat. Sol.(b)* **243**, 3629 (2006).
- ²³ O. Gunawan, Y.P. Shkolnikov, K. Vakili, T. Gokmen, E. P. De Poortere, and M. Shayegan, *Phys. Rev. Lett.* **97**, 186404 (2006).
- ²⁴ O. Gunawan, T. Gokmen, K. Vakili, M. Padmanabhan, E. P. De Poortere, and M. Shayegan, *Nature Phys.* **3**, 388 (2007).
- ²⁵ T.J. Gramila, J.P. Eisenstein, A.H. MacDonald, L.N. Pfeiffer, and K. W. West, *Phys. Rev. Lett.* **66**, 1216 (1991); U. Sivan, P.M. Solomon, and H. Shtrikman, *Phys. Rev. Lett.* **68**, 1196 (1992); M.P. Lilly, J.P. Eisenstein, L.N. Pfeiffer, and K. W. West, *Phys. Rev. Lett.* **80**, 1714 (1998); R. Pillarisetty, Hwayong Noh, D. C. Tsui, E. P. De Poortere, E. Tutuc, and M. Shayegan, *Phys. Rev. Lett.* **89**, 016805 (2002).
- ²⁶ M. Kellog, J.P. Eisenstein, L.N. Pfeiffer, K.W. West, *Phys. Rev. Lett.* **93**, 036801 (2004); E. Tutuc, M. Shayegan, D.A. Huse, *Phys. Rev. Lett.* **93**, 036802 (2004); J.P. Eisenstein and A.H. MacDonald, *Nature* **432**, 691 (2004).
- ²⁷ G.S. Boebinger, H.W. Jiang, L.N. Pfeiffer, and K.W. West, *Phys. Rev. Lett.* **64**, 1793 (1990); A. Sawada, Z.F. Ezawa, H. Ohno, Y. Horikoshi, Y. Ohno, S. Kishimoto, F. Matsukura, M. Yasumoto, and A. Urayama, *Phys. Rev. Lett.* **80**, 4534 (1999).
- ²⁸ V.S. Khrapai, E.V. Deviatov, A.A. Shashkin, V.T. Dolgoplov, F. Hastreiter, A. Wixforth, K.L. Campman, and A.C. Gossard, *Phys. Rev. Lett.* **84**, 725 (2000).
- ²⁹ I.R. Pagnossin, A.K. Meikap, T.E. Lamas, G.M. Gusev, and J.C. Portal, *Phys. Rev. B* **78**, 115311 (2008).
- ³⁰ G.M. Minkov, A.V. Germanenko, O.E. Rut, O.I. Khrykin, V.I. Shashkin, and V.M. Daniltsev, *Nanotechnology* **11**, 406 (2000).
- ³¹ G.M. Minkov, A.V. Germanenko, O.E. Rut, A.A. Sherstobitov, A.K. Bakarov, and D.V. Dmitriev, *Phys. Rev. B* **82**, 165325 (2010).
- ³² G. M. Minkov, A. V. Germanenko, O. E. Rut, A. A. Sherstobitov, A. K. Bakarov, and D. V. Dmitriev, arxiv: 1101.5869.
- ³³ B.L. Altshuler and A.G. Aronov, in *Electron-Electron Interactions in Disordered Conductors*, ed. A.J. Efros and M. Pollack, Elsevier Science Publishers, North-Holland, 1985.
- ³⁴ B.N. Narozhny, Gabor Zala, and I.L. Aleiner, *Phys. Rev. B* **65**, 180202 (2002)
- ³⁵ L.D. Landau, E.M. Lifshitz, *Quantum mechanics*, Course of Theoretical Physics, vol. 3, Pergamon, 1991.
- ³⁶ I.V. Gornyi, A.G. Yashenkin, and D.V. Khveshchenko, *Phys. Rev. Lett.* **83**, 152 (1999).
- ³⁷ In the experiments of Refs. [31,32] the random potential was created by charged impurities situated near $z = 0$. In this case the range of W is determined by 3D screening length $d_W \sim 1/\sqrt{z k_F}$. In order to consider this random potential as short-ranged the following condition $d_W \ll l$ or, equivalently, $k_{Fl} \gg \sqrt{k_F/z}$ should hold.
- ³⁸ D. Belitz and T.R. Kirkpatrick, *Rev. Mod. Phys.* **66**, 261 (1994).
- ³⁹ G. Zala, B.N. Narozhny, and I.L. Aleiner, *Phys. Rev. B* **64**,

- 214204 (2001).
- ⁴⁰ A. Kamenev and Y. Oreg, Phys. Rev. B **52**, 7516 (1995).
- ⁴¹ K. Flensberg, B. Yu-Kuang-Hu, and A.-P. Jauho, J.M. Kinaret, Phys. Rev. B **52**, 14716 (1995).
- ⁴² B.L. Altshuler, A.G. Aronov, A.I. Larkin, D.E. Khmel'nitskii, Zh. Éksp. Teor. Fiz. **81**, 768 (1981) [Sov. Phys. JETP **54**, 411 (1981)].
- ⁴³ B.L. Altshuler and A.G. Aronov, Pis'ma Zh. Éksp. Teor. Fiz. **33**, 515 (1981) [JETP Lett. **33**, 499 (1981)].
- ⁴⁴ B.L. Altshuler, D.E. Khmel'nitskii, A.I. Larkin, and P.A. Lee, Phys. Rev. B **22**, 5142 (1980).
- ⁴⁵ F. Wegner, Z. Phys. B **35**, 207 (1979); L. Schaefer and F. Wegner, Z. Phys. B **38**, 113 (1980); A.J. McKane and M. Stone, Ann. Phys. (N.Y.) **131**, 36 (1981); K.B. Efetov, A.I. Larkin, D.E. Khmel'nitskii, Sov. Phys. JETP **52**, 568 (1980).
- ⁴⁶ A.M.M. Pruisken, M.A. Baranov, and B. Škorić, Phys. Rev. B **60**, 16807 (1999);
- ⁴⁷ C. Castellani and C. Di Castro, Phys. Rev. B **34**, 5935 (1986).
- ⁴⁸ A. Kamenev and A. Andreev, Phys. Rev. B **60**, 2218 (1999).
- ⁴⁹ C. Castellani, C. Di Castro, P.A. Lee, M. Ma, S. Sorella, and E. Tabet, Phys. Rev. B **33**, 6169 (1986).
- ⁵⁰ D.J. Amit, *Field theory, renormalization group, and critical phenomena*, (World Scientific, 1984).
- ⁵¹ A. Schmid, Z. Phys. **271**, 251 (1974); B.L. Altshuler and A.G. Aronov, JETP Lett. **30**, 482 (1979).